



1 **Seasonal variation of mercury concentration of ancient olive**
2 **groves of Lebanon.**

3

4 Nagham Tabaja^{1,2,3}, David Amouroux⁴, Lamis Chalak², François Fourel⁵, Emmanuel Tessier⁴,
5 Ihab Jomaa⁶, Milad El Riachy⁷, Ilham Bentaleb¹

6

7 ¹ ISEM, Univ Montpellier, CNRS, IRD, Montpellier, France

8 ² Faculty of Agronomy, Plant Production Department, The Lebanese University, Dekwaneh, Lebanon

9 ³ Plateforme de Recherche et d'Analyses en Sciences de l'Environnement (PRASE), Ecole Doctorale de Sciences et
10 Technologie, Université Libanaise, Hadath, Liban

11 ⁴ Université de Pau et des Pays de l'Adour, E2S/UPPA, CNRS, Institut des Sciences Analytiques et de Physico-Chimie
12 pour l'Environnement et les Matériaux (IPREM), PAU, France

13 ⁵ UMR CNRS 5023 LEHNA, Université Claude Bernard Lyon 1, Villeurbanne, France

14 ⁶ Department of Irrigation and Agrometeorology, Lebanese Agricultural Research Institute (LARI), P.O. box 287,
15 Zahle, Lebanon

16 ⁷ Department of Olive and Olive Oil, Lebanese Agricultural Research Institute (LARI), P.O. box 287, Zahle, Lebanon

17

18 *Correspondence to:* Ilham Bentaleb (Email: ilham.bentaleb@umontpellier.fr, Tel: +33(0) 6 38 61 57 69

19

20



21 **Abstract.** This study aimed to investigate the olive, an iconic tree of the Mediterranean basin, seasonality of (Hg)
22 mercury pollution. Hg concentrations of foliage, stems, soil surface, and litter was analyzed on monthly basis in
23 ancient olive trees growing in two groves in Lebanon, Bchaaleh and Kawkaba (1300 and 672 m.a.s.l respectively). A
24 significantly lower concentration was registered in stems (~7-9 ng/g) with respect to foliage (~35-48 ng/g) in both
25 sites with the highest foliage Hg concentration in late winter-early spring and the lowest in summer. It is noteworthy
26 that olive fruits also have the lowest Hg concentration (~7-11 ng/g). The soil has the highest Hg content (~62-129
27 ng/g) likely inherited through the cumulated litter biomass (~ 63-76 ng/g). A good covariation observed between our
28 foliage Hg time-series analysis and those of pCO₂ and Hg concentrations of the atmospheric Northern hemisphere
29 confirms that mercury pollution can be studied through olive trees. More precisely, spring sampling is recommended
30 if the objective is to assess the tree's susceptibility to Hg uptake. This may draw an adequate baseline for global
31 inventories on Hg vegetation uptake and new studies on olive trees in the Mediterranean to reconstruct regional Hg
32 pollution concentrations in the past and present.

33 **Keywords:** Eastern Mediterranean, ancient groves, *Olea europaea* L., mercury pollution, plant tissues, soil and litter

34

35



36 1. Introduction

37

38 Mercury (Hg) is among the most common heavy metals polluting the Earth (Briffa et al. 2020). It is found as all heavy
39 metals naturally on the Earth's crust reservoir and in the atmosphere through the natural long-term Hg biogeochemical
40 cycle (i.e., volcanic activities, geological weathering). This metal is easily modified into several oxidation states and
41 it can also be spread through many ecosystems (Boening 2000). The natural Hg cycle has been modified due to
42 anthropogenic activities (i.e., mining, smelting, soil erosion due to deforestation, gold extraction, agriculture-
43 fertilizers, manure) (Patra and Sharma 2000). Among natural and anthropogenic Hg emissions, inorganic elemental
44 Hg (Hg(0)) is the most dominant chemical form. It is generally transferred through the atmosphere by the winds and
45 mass air. This highly diffusive Hg can easily pass biological barriers (i.e. cell membranes, foliage, skin) and bind
46 covalently with organic groups forming the widespread toxic methylmercury (MeHg, CH₃Hg⁺) (Clarkson and Magos
47 2006). Anthropogenic activities endorse an accumulation of heavy metals in terrestrial and aquatic ecosystems. This
48 can remain for over 100 years after the closure of the pollution source. The exchange between the Hg amount in the
49 soil and uptake of the Hg by the plants is not stable and is variable dependent (e.g. cation-exchange capacity, soil pH,
50 soil aeration, and plant species) (Patra and Sharma 2000).

51 Large forests with large foliage surface area are known to act as a sink of atmospheric Hg in the ecosystem. Plant
52 foliage take up Hg deposited on leaf surfaces through the stomata (ie. Photosynthesis) and leaf cuticles (Hanson et al.
53 1995; Jiskra et al. 2018; Li et al. 2017; Lodenius et al. 2003; Maillard et al. 2016; Rea et al. 2002; Yanai et al. 2020)
54 where it accumulates with minimal mobility and small portions released back into the atmosphere or transfers the Hg
55 through the other plant organs (Cavallini et al. 1999; Hanson et al. 1995; Li et al. 2017; Lodenius et al. 2003; Schwesig
56 and Krebs 2003). Water and soil are another uptake Hg source through roots (Bishop et al. 1998; Li et al. 2017). These
57 two Hg absorption pathways in plants are also described in Hg contaminated sites on several plant species reporting
58 the accumulation of Hg in the foliage and also in the roots where Hg can be absorbed through xylem sap (Assad et al.
59 2017). Tree's Hg is transferred to the forest floor through litter and throughfall and hence passes to the soil (Rea et al.
60 1996). Litter is said to constitute 30 to 60 % of the Hg atmospheric deposition in Europe and North America forests
61 (Rea et al. 1996; Blackwell and Driscoll 2015; Zhou et al. 2018). The Hg input through the litter is greater than the
62 input from that of the wet deposition (Wang et al., 2016). The Litter Hg is the dominant pathway in forests where it
63 contributes to 53 and 90 % of the dry deposition to the forest (Wright et al., 2016).

64 In earth ecosystem, soil as part of the geological reservoir has naturally the highest Hg reservoir (D. Obrist et al., 2018;
65 O'Connor et al., 2019) followed by trees (Yang et al. 2018). This Hg is provided by natural geological sources and
66 natural events such as forest fires, volcanic eruptions (Ermolin et al. 2018; Obrist et al. 2018; O'Connor et al. 2019)
67 and anthropogenic sources (UNEP, 2019). In return, soil and plants can reemit Hg to the atmosphere through diffusion
68 and transpiration during photo-respiration biological processes (Luo et al., 2016; Yang et al., 2018a; Assad, 2017;
69 Schneider et al., 2019; Gworek et al., 2020). Trees are hence important drivers of Hg between the atmosphere and the
70 soil (Yang et al. 2018) .

71 The studies of the Hg cycle in forest ecosystems show that gaseous elemental Hg(0) is the main source taken up by
72 plants (Bishop et al. 2020; Zhou et al. 2021). Differences are observed between ecological functional traits and species
73 among other factors. Hg in tree rings is also analyzed usually to determine if the Hg concentration are influenced more



74 by the soil Hg concentration or by the atmospheric Hg deposition. This atmospheric deposition that has declined in
75 recent decades can be shown in the declining concentration from the older to newer tree rings suggesting a more
76 important uptake through the foliage than the roots. Hg dendrochemistry can help investigate Hg past impacts on
77 terrestrial ecosystems and also help predict future changes in the cycle of Hg in forests (Yanai et al., 2020). The recent
78 studies on Hg uptake by vegetation have highlighted the importance of the role of different parameters as vapor
79 pressure deficit, soil water content, climatic conditions, date of sampling, leaf mass area, tree functional groups,
80 stomatal conductance affecting potentially the root uptake of Hg dissolved in soil water and the absorption rate via
81 stomata and eventually the Hg leaf content (Blackwell & Driscoll, 2015; Rea et al., 2002; Wohlgemuth et al., 2021;
82 Yang et al., 2018b).

83 Analysis of long term atmospheric Hg(0) and CO₂ concentrations are very informative to understand the role of the
84 vegetation in the global Hg cycle (Jiskra et al. 2018). Studies conducted in temperate Northern Hemisphere (44°N)
85 show strong atmospheric Hg(0) seasonal variation, with high values in winter and low values in summer (Jiskra et al.
86 2018). These authors show also a significant positive correlation between the monthly Hg(0) and CO₂ concentrations.
87 They highlighted a one-month offset in Hg(0) summer time minima happening in September in comparison to the CO₂
88 minima value occurring in August, this trend is not observed in winter time. The uptake of Hg(0) by the vegetation
89 continues during CO₂ respiration periods during the fall and night when the ecosystem exchange of CO₂ turns from
90 being a sink to becoming a source (Jiskra et al. 2018; Wofsy et al. 1993).

91 The total gaseous Hg (TGM) in the Mediterranean atmosphere is similar to Northern Europe (1.3 to 2.4 ng m⁻³) (Kotnik
92 et al. 2014). In the case of a semi-closed sea such as the Mediterranean basin with warm summers, high sea-water
93 evaporation, solar radiations and Hg anthropogenic sources, the Mediterranean Sea is acting as a net source of Hg to
94 the global atmosphere (Kotnik et al. 2014) making the Mediterranean an air-pollution area (Baayoun et al. 2019;
95 Borjac et al. 2019).

96 The olive tree (*Olea europaea* L.) is one of the most distinctive Mediterranean agro-ecosystems tree species, and is
97 adapted to drought (Sghaier et al. 2019). Considered among the oldest trees in the Mediterranean basin, these
98 centennial olive trees are still growing in many countries along both the eastern and western shore, surviving to various
99 stresses and witnessing the historical, cultural and ecological importance of this tree (Terral et al. 2004). On the other
100 hand, the olive tree remains a key component of agriculture today and in the future. Therefore, it is important to
101 understand the on-site behavior of the olive tree to Hg pollution in its natural Mediterranean growing environment.

102 The Hg source in foliage varies with respect to the amount of contamination. In polluted sites the soil is the main
103 source of Hg while away from those sites the atmosphere is the most important source (Naharro et al. 2018).

104 Lebanon, a small country at the Eastern Mediterranean, is facing important anthropogenic pressure within a changing
105 environment (Gérard and Nehmé 2020). The air quality in Lebanon all over the country is noted to be moderately
106 unsafe with an annual mean concentration of 31 µg/m³ of PM 2.5 which is above the maximum recommended value
107 (10 µg/m³) (Lebanon: Air Pollution IAMAT 2020). Adding to that, soil samples collected from different areas in
108 southern Lebanon showed values of Hg concentration ranging between 160-6480 ng/g (Borjac et al. 2020). The main
109 contributors of the air pollution include cement industries, mineral and chemical factories, vehicles emissions, food



110 processing and oil refining. Ancient olive groves are found across different agroclimatic areas at different altitudinal
111 belts, still producing agricultural outcomes and consumed, coping with these various pollution pressures.
112 In this study, remote sites were investigated for possible Hg contamination that is expected to be very low, since the
113 atmospheric Hg is still deposited in remote areas (Grigal, 2003). This is due to the surrounding polluted sites and the
114 transfer of pollution through wind and the Mediterranean Sea to other areas. In addition to the lack and scarcity of
115 studies on Hg pollution in the Eastern Mediterranean. The aim was to follow monthly concentrations variation of Hg
116 during two consecutive years 2019-20 in the foliage and stems of olive trees, soils and litter of two ancient groves of
117 Lebanon known to be over 1400 years old (Yazbeck et al., 2018). Specifically, two main objectives are taken into
118 account: 1) How does Hg content vary seasonally in uncontaminated and remote sites? 2) Is Hg-uptake from the soil
119 to the foliage low in uncontaminated sites?
120

121 **2. Materials and methods**

122
123 Two monumental olive groves were chosen in the context of their historical and agricultural importance, since these
124 two sites are considered to contain olive trees of an age older than 1400 years old still providing till this date an
125 agricultural outcome that is consumed.

126 **2.1. Geographic setting and environmental context**

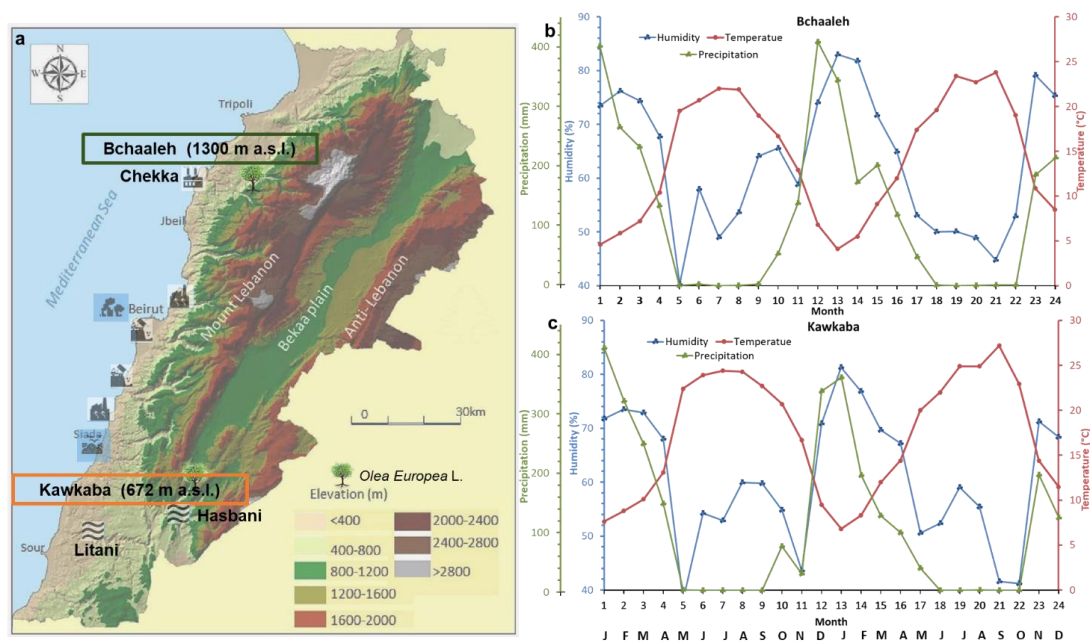
127 128 **2.1.1. Bchaaleh site (BC) - North Lebanon**

129
130 This grove is situated in Batroun district (Latitude 34°12'06'' N, Longitude 35°49'23'' E, Altitude 1300 m.a.s.l.)
131 (Figure 1a). Olive trees are growing rainfed in a sandy loam texture soil of grain size analysis of sand, silt and clay
132 percentages are 52.8 %, 38.7 % and 10.7 % respectively. Soil pH is 7.07 ± 0.26 with organic matter and calcium
133 carbonate contents are 1.7 % and 38.3 % respectively (Yazbeck et al. 2018). In this study, soil profiles of carbon and
134 nitrogen contents were analyzed. Organic carbon contents decreased with soil depth from about 4 % at 0-1 cm (Soil
135 surface) to 2.7 % at 30-60 cm. The total nitrogen is about 0.3 % at 1cm depth and 0.2 % at 30-60 cm depth. The olive
136 trees are located on two terraces. The first terrace is at 1.5 meter above the road level while the second is at the road
137 level. They are maintained by the municipality since the last four decades as an endowment property. Precipitation
138 average ranges between 229 and 392 mm/year in winter and between zero and less than 2 mm/year in summer, while
139 average temperature is between 4 and 8 °C in winter and between 20 and 23 °C in summer (data extracted from LARI
140 climatic data) (Figure 1b, Table S1).

141 The village is at about 36 km from Chekka town located at a lower altitude (0-200 m.a.s.l.) nearby the sea (Figure 1a),
142 and which is classified as a source of air pollution (EJOLT 2019). Chekka hosts an important national cement factory
143 responsible of carbon dioxide, sulfur dioxide, nitrous oxides, monoxide and particulate material emissions causing
144 respiratory and health issues (Kobrossi et al. 2002) and water pollution (Nassif et al. 2016). At 28 km from BC, the
145 small commercial port of Selaata (0-37 m.a.s.l.) that emits many pollutants (ie. Phosphogypssum, heavy metals,
146 radionuclides) expanded via water and air pathways (Petrlik et al. 2013; Yammine et al. 2010). As dissolved gaseous



147 Hg from natural and human activities is saturated in the upper Eastern Mediterranean Sea, Gårdfeldt et al., (2003)
 148 have evidenced that Mediterranean Sea is a source of airborne elemental Hg.
 149



150
 151 **Figure 1.** (a) Site locations of the two selected focus areas (modified after Shared Water Resources of Lebanon, Nova
 152 Science Publishers 2017). (b,c) Climatic data of Precipitation, Temperature and Humidity collected from the
 153 meteostations installed by LARI between 2009 and 2018 (Colors should be used for this figure in print)
 154

155 **2.1.2. Kawkaba site (KW) - South Lebanon**

156
 157 The second grove is located in the village of Kawkaba (KW), South Lebanon (Latitude 33°23'856'' N, Longitude
 158 35°38'588'' E, Altitude 672 m.a.s.l. (Figure 1a). KW soil is characterized as clay loam soil of pH 7.5 ±0.5. Soil organic
 159 material and calcium carbonate average are 1.7 % and 59.0 % respectively (Al-Zubaidi et al. 2011) and grain size
 160 analysis of sand, silt and clay percentages are 6 %, 28 % and 66 % respectively. The analysis of organic carbon and
 161 nitrogen at the 0-1 cm and at 1-30 cm decrease from about 9.0 % to 2.2 % and from 0.9 % to 0.3 % for the carbon and
 162 nitrogen respectively. Average precipitation ranges between 215 and 374 mm/year in winter and drop to almost zero
 163 mm in summer, while average temperature is between 7 and 11 °C in winter and between 21 and 27 °C in summer
 164 (data extracted from LARI climatic data) (Figure 1c, Table S1).

165 The village has to its east the Hasbani river, originated from the north-western slopes of Mount Hermon in Hasbaya
 166 (36 km away from KW and located at 750 m.a.s.l.) (Badr et al. 2014; Jurdi et al. 2002). On the other hand, the Litani
 167 River (170 km long and located at 800 to 1000 m.a.s.l.) (Figure 1a) rising in the south of the Bekaa valley is about 29
 168 km away from KW (Abou Habib et al. 2015, Khatib et al. 2018). These two rivers are polluted and for these reasons



169 they are not used for irrigating crops in KW and surrounding areas while the olive trees are growing rainfed as per
170 indicated by the municipality of KW.

171 Climatic data in both BC and KW were collected from meteorological station and manual rain gauge installed in the
172 villages by LARI (Lebanese Agricultural Research Institute) (Figure 1b,c). CO₂ data used in this study are from NOAA
173 Global Monitoring Laboratory (https://gml.noaa.gov/webdata/ccgg/trends/co2/co2_trend_gl.txt).

174

175 **2.2. Field sampling**

176

177 For the Hg concentration analysis, four olive trees of 8 to 15 m foot circumference (and the average height of the trees
178 4-6m) were sampled in each of the two groves, within BC two trees taken in an upper terrace (BCO1-Bchaaleh-Tree
179 1, BCO4-Bchaaleh-Tree 4) and two other trees in a 1.5 m lower terrace (BCO9-Bchaaleh-Tree 9, BCO12-Bchaaleh-
180 Tree 12) (Figure S1). For Hg analysis, foliage, stems and fruits were collected from the trees, while litter and soil were
181 sampled directly under the trees, starting from February 2019 and ending by September 2020. For each olive tree,
182 both sun exposed and shaded foliage (olive tree bears foliage from three different years) and stems (terminal portions
183 of 20 cm) with no evidence of pathogens were randomly taken and merged from the upper, middle, and lower canopy
184 position of the olive trees on a monthly basis using a manual pruner. Litter and soil surface were separately collected
185 on the whole top surface area of the olive groves and stored in different paper bags once every four months. In parallel,
186 soil sampling was performed using a bucket auger to a maximum depth of 60cm. These soil samples were collected
187 from around the whole olive grove in order to be a good representative of the whole site. In both sites, the soil showed
188 uniform color and texture. Soil cores were fractioned in soil surface (0-1 cm), 1 to 30 cm depth and from 30 to 60 cm
189 depth in order to study the effect and accumulation of Hg concentration on the different depth layers. To avoid
190 contamination, gloves were worn while collecting samples, and the equipment was rinsed with methanol between
191 every sample. A set of 453 samples were collected and stored in paper bags until further preparation for the Hg
192 analysis.

193

194 **2.3. Sample preparation for Hg analysis**

195

196 Collected foliage and stems were rinsed with distilled water and then dried for 48 hours in an oven at a temperature
197 of 60°C at maximum. The dried foliage, stems, litter and olive fruits samples were grinded using an electrical stainless
198 grinding machine with no heating system for 5-10 minutes, while soil samples were prepared with a manual natural
199 agate grinder. All samples were later sieved using an inox stainless-steel 125-micron sieve mesh to collect
200 homogeneous powders for analysis. A total of 150 mg for foliage and soil (50 mg/analysis), and 300 mg of litter and
201 stems (100 mg/analysis) were considered in triplicates for analysis of Hg concentrations.

202

203 **2.4. Analytical method**

204

205 For the Hg elemental analysis, a total of 453 powder samples from foliage, stem, grain, litter and soil were analyzed
206 using an advanced Hg analyzer AMA 254 (Altec) as described elsewhere (Barre et al. 2018; Duval et al. 2020). A



207 known amount of sample (50-100 mg) is weight in a nickel boat, using a 10^{-6} g precision balance. The sample aliquot
208 is first dried at 120°C for 60s and subsequently pyrolyzed at 750°C for 150s, under oxygen flow. The resulting gaseous
209 Hg produced during the sample decomposition is amalgamated on a gold trap and then released to an Atomic
210 Absorption spectrometer after a thermal desorption step at 950°C . The AMA 254 instrument was calibrated through
211 several external matrix-matched calibration procedures using the following certified reference materials: IAEA-456
212 sediment (77 ± 5 ng Hg/g), NIST-1575A pine needles ($39,9 \pm 0,7$ ng Hg/g) and IAEA336 (200 ± 40 ng Hg/g). The
213 QA/QC evaluation of the analytical procedure was completed with a continuous monitoring of the blank's values
214 (Nickel boat Hg background noise), every 15 analyzed samples. The precision of the measurements was assessed
215 through replicated analyses ($n=2$) of 13 % of the total amount of samples ($n=453$). Average relative standard deviations
216 of 5 % and 2.5 % are thus associated to the reported Hg concentrations for the 2019 and 2020 samples batches,
217 respectively. The detection limit of the analytical method has been assessed to 0,7 ng Hg/g, for analytical sessions.
218 Subsamples of soil were used for carbon and nitrogen elemental contents (%) analysis. A 2 mg (acid washed soil and
219 bulk soil) of powders were weighed into tin capsules and measured by dry combustion using a Pyrocube Elemental
220 Analyser (EA, Elementar GmbH).

221

222 **2.5. Statistical analysis**

223

224 R 4.1.0 program was used for the statistical analysis, the data in not normally distributed. For the effect of tissue type
225 on Hg concentration, Wilcoxon test was used with the tissue type (foliage and stems) as the main effect. Pearson
226 correlation analysis was used to examine the inter-individual correlation of Hg concentration between the trees.
227 Correlation between Hg concentration of soil surface, litter and foliage was studied using a correlation test. For the
228 seasonal effect (Winter: Mid-December till Mid-March, Spring: Mid-March till Mid-June, Summer: Mid-June till
229 Mid-September, Autumn: Mid-September till Mid-December) on Hg concentration, Wilcoxon test was used
230 considering the unequal data available for the different seasons. Finally, the effect of climatic factors (Temperature,
231 precipitation, $p\text{CO}_2$) on Hg accumulation was examined using a Wilcoxon test.

232

233 **3. Results**

234

235 **3.1. Hg concentrations in plant tissues, litter and soil at BC and KW groves**

236

237 Hg concentrations varied generally according to both tree tissues and groves agroclimatic conditions (Table 1, Figure
238 1). Hg values in the foliage varied significantly between the two groves ($p\text{-value}=1.581*10^{-6}$), where the highest
239 concentration was recorded in BC (48.1 ± 10.6 ng/g) vs. (35 ± 12.4 ng/g) in KW. Soil surface also recorded a difference
240 in Hg concentration between BC and KW, with 61.9 ± 20.0 ng/g in BC and 128.5 ± 9.4 ng/g in KW. Soil 0-30 cm
241 samples taken from BC and KW groves, values ranged between 31.8 ± 4.7 ng/g and 70.2 ± 23.4 ng/g respectively. In
242 soil 30-60 cm Hg concentrations recorded 19.5 ± 6.73 ng/g at BC. No significant differences were recorded for litter
243 and stems Hg concentrations ($p\text{-value}=0.0915$ and $p\text{-value}=0.2215$ respectively) between the groves, with litter values
244 of 62.9 ± 17.8 at BC and 75.7 ± 20.3 ng/g at KW vs. stem values of 7.9 ± 2.8 ng/g at BC and 9.0 ± 4.7 ng/g at KW.



245 Positive correlations were observed between soil and litter in BC ($r=0.60$) and KW ($r=0.95$) though statistically
 246 insignificant (p -value= 0.40 and 0.13 respectively).

247 In descending order of Hg concentrations and considering the different sites, plant tissue, soil and litter samples, the
 248 Hg concentrations could be ranked in BC, soil surface > litter > foliage > soil 0-30 cm > soil 30-60 cm > stems; and in
 249 KW, soil surface > litter > soil 0-30 > foliage > soil 30-60 > stems (Table 1).

250

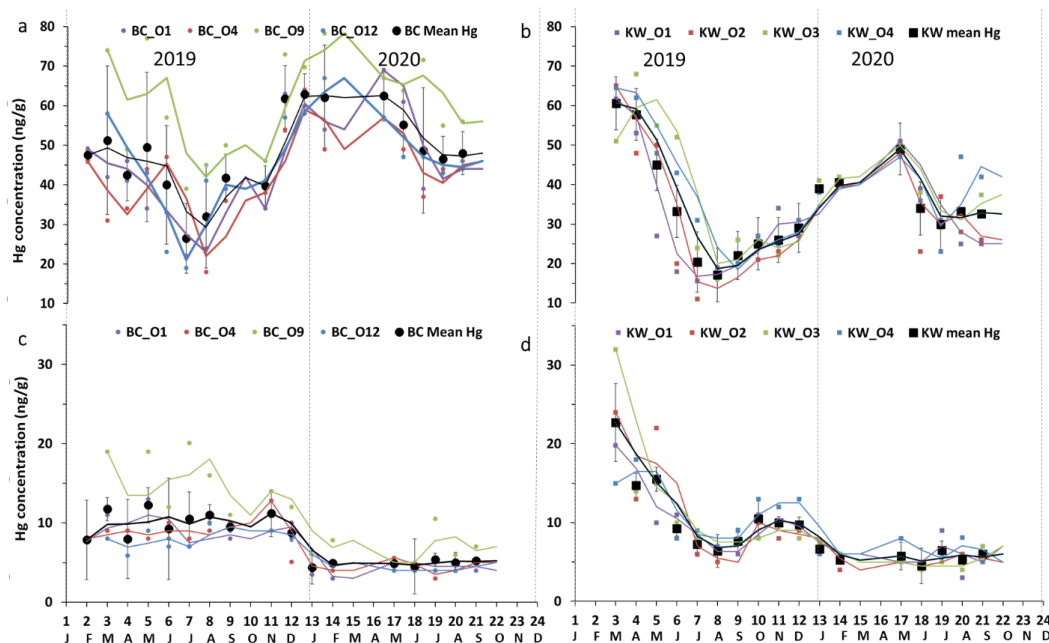
251 **Table 1.** Overall mean values of Hg concentration (ng/g) of the different studied material in both BC and KW olive
 252 groves

	Bchaaleh (BC)			Kawkaba (KW)		
	Average (ng/g)	SD	N	Average (ng/g)	SD	N
Foliage	48.1	10.6	66	35.0	12.4	67
Stems	7.9	2.8	66	9.0	4.7	67
Litter	62.9	17.8	7	75.7	20.3	6
Soil Surface	61.9	20.0	8	128.5	9.4	6
Soil 0-30cm	31.8	4.7	6	70.2	23.4	5
Soil 30-60cm	19.5	6.7	5	28.0		1
Fruit	7.0	3.5	3	11.0		1

253

254

255



256

257

258

259

260

Figure 2. Seasonal variations of foliage Hg concentration in (a) BC and (b) KW olive groves and stems Hg concentration in (c) BC and (d) KW olive groves.



261 **3.2. Seasonal variation of Hg concentration**

262
 263 Hg concentrations recorded between February 2019 and September 2020 reflected a significant seasonal variation in
 264 both sites ($p\text{-value} < 2.2 \times 10^{-16}$). In BC grove, foliage registered its highest Hg concentration during winter and spring
 265 with 61.8 ± 7.6 ng/g and 55.1 ± 12.5 ng/g respectively, and its lowest Hg amount during summer and autumn with
 266 41.5 ± 12.7 ng/g and 44.4 ± 6.2 ng/g, respectively. Seasonal effect on foliage and stems ($p\text{-value} < 2.2 \times 10^{-16}$), the lowest
 267 Hg concentration values for all the mentioned samples were registered during winter. The stems and soil 0-30cm
 268 highest values was registered in autumn (Table 2). Significant differences were found in foliage Hg values between
 269 summer and winter ($p\text{-value} = 0.00020$), and autumn and winter ($p\text{-value} = 0.00014$). Similarly, stems Hg values varied
 270 significantly between spring and winter ($p\text{-value} = 0.030$), autumn and winter ($p\text{-value} = 0.047$). In KW, the highest Hg
 271 concentrations for foliage and stems were registered in spring with 51.8 ± 4.5 ng/g, 11.7 ± 6.7 ng/g respectively.
 272 Significant differences were found in foliage Hg values between summer and winter ($p\text{-value} = 0.013$), autumn and
 273 winter ($p\text{-value} = 0.00067$), autumn and spring ($p\text{-value} = 1.589 \times 10^{-05}$), spring and winter ($p\text{-value} = 9.383 \times 10^{-05}$) and
 274 spring and summer ($p\text{-value} = 2.327 \times 10^{-06}$). Similarly, stems Hg values varied significantly between spring and winter
 275 ($p\text{-value} = 0.006$), spring and summer ($p\text{-value} = 0.0036$) and autumn and spring ($p\text{-value} = 0.011$). A seasonal variation
 276 is observed in both olive groves especially in the foliage and also between the two groves location.

277

278 **Table 2.** Seasonal mean Hg concentration (ng/g) and standard deviations seasonal variation of the different studied
 279 material in both BC and KW olive groves. Grey color indicated the highest Hg concentration values among the
 280 different elements during the different seasons

Hg (ng/g)												
Bchaaleh	Spring	SD	N	Summer	SD	N	Autumn	SD	N	Winter	SD	N
Foliage	55.1	12.5	16	41.5	12.7	24	44.4	6.2	12	61.8	7.6	18
Stems	7.8	3.8	16	7.61	3.9	24	8.3	2.7	12	6.4	2.9	18
Litter	79.3	26.5	3	64.7	4	4	55.5		2	48.6	13.3	3
Soil Surface	58.3	13	3	84.5	21.2		50		3	50.6	23.5	3
0-30cm	33.6	6.2	2	32.2	4.3		34.5		2	27	0.7	3
30-60cm	23.1	9.1	2	20.7			19.6		2	11		1
Kawkaba	Spring	SD	N	Summer	SD	N	Autumn	SD	N	Winter	SD	N
Foliage	51.8	4.5	16	28	7.2	24	28.5	7.2	16	33.9	5.6	18
Stems	11.7	6.7	16	6.5	1.4	24	7.7	2.1	16	6.9	1.6	18
Litter	90.1	29.3	2	67	24	2	70	1.4	2			
Soil Surface	132	8.5	2	118	4.2	2	135.6	2.2	2			
0-30cm	57.9	11.2	2	65.8		1	84.8	36.4	2			
30-60cm	28		1									

281

282 **3.3. Tree comparison**

283
 284 In the upper terrace of BC grove, the foliage and stems average Hg concentration per tree ranked respectively between
 285 44.6 ± 13.3 ng/g and 7.1 ± 2.9 ng/g for BCO1 and between 42.4 ± 11.5 ng/g and 7.0 ± 2.8 ng/g for BCO4. In the lower
 286 terrace of the same site, Hg concentrations were found respectively between 60.7 ± 12.7 ng/g and 11.2 ± 5.2 ng/g for
 287 BCO9 and between 45.6 ± 12.7 ng/g and 6.4 ± 2.2 ng/g for BCO12 (Figure 2a,c).



288 In KW grove, trees show no significant difference for both foliage and stems. The average concentration per tree in
289 foliage and stems were 32.4 ± 12.2 ng/g and 8.5 ± 4.0 ng/g respectively for KWO1, 32.8 ± 14.7 ng/g and 8.9 ± 6.0
290 ng/g for KWO2, 37.6 ± 14.0 ng/g and 9.3 ± 6.7 ng/g in KWO3 and 37.7 ± 13.6 ng/g and 9.6 ± 4.0 ng/g in KWO4
291 (Figure 2b,d).

292 In BC grove, the trees located on the lower terrace recorded higher Hg concentration values than those of the upper
293 terrace especially tree 9. While KW grove had similar Hg concentration among all four trees.

294

295 **3.4. Hg concentration and agro-climatic effect**

296

297 The Wilcoxon test for a non-normal distribution between Hg concentration of foliage and stems and temperature
298 shows no significant effect with a 0.013 p-value. While a significant effect was found between Hg concentration of
299 foliage and stems, precipitation, relative humidity and atmospheric CO₂ (pCO₂) (p-value $2.2 \cdot 10^{-16}$, $5.60 \cdot 10^{-10}$ and 2
300 $\cdot 10^{-16}$ respectively). A positive correlation was found between the precipitation and Hg concentrations of foliage and
301 stems, where values increased with higher precipitation and lower temperature records. In dryer seasons, starting from
302 May to mid-October, the Hg concentration of foliage decreased with the increase of temperature and the decrease of
303 the precipitation for all studied elements.

304

305 **4. Discussion**

306

307 **4.1. Hg concentration in plant tissues, soil and litter in the studied groves**

308

309 In both groves our values showed a larger Hg concentration in the olive foliage (BC average of 48.1 ± 10.6 ng/g; KW
310 average of 35.0 ± 12.4 ng/g), than that of stems (BC average of 7.9 ± 2.8 ng/g; KW average of 9.0 ± 4.7 ng/g) and that
311 of olive fruits (7 ± 3.5 ng/g at BC, n=3 and 11 ng/g in KW, n=1). Our data corroborates previous studies (Bargagli
312 1995; Higuera et al. 2016; Naharro et al. 2018) showing that olive foliage has the main Hg content among analyzed
313 plant tissue. Moreover, we demonstrate that our values are lower than 200 ng/g considered as Hg pollution threshold
314 (Kabata-Pendias and Pendias 2000) and confirm no pollution effect for both BC and KW groves (Table S2; Figure
315 S2a,b). This been said, our sites are good remote bioindicators of the uptake of Hg through the plant although more
316 prolonged time range is needed. Hg in foliage originates predominantly from the air, and it can be delivered to the soil
317 through the litter (Tomiyasu et al. 2003). Adding to that, the atmospheric Hg uptake in foliage dominates over Hg
318 release (Pleijel et al., 2021). Since normally the main source of Hg into the foliage is atmospheric and minimally
319 through the soil, this explains the higher Hg concentration in the foliage, while in the stems the main uptake is from
320 the soil and it seems to be minimal (Tomiyasu et al., 2005) explaining the much lower level of Hg concentration in
321 the stems than that in the foliage.

322 The soil surface and litter registered the highest Hg concentration (62 to 129 ng/g) among all samples (foliage, stems,
323 fruit) in both groves (Table 1) suggesting that the soil is the main Hg reservoir through the Hg throughfall and litter
324 inputs. Our findings are in agreement with studies on evergreen forest ecosystems reporting that soil can hold more
325 than 60 % of Hg input to the forest floor (Wang et al. 2016). Our soil surface sites values (61.9 ± 20.0 ng/g in BC and



326 128.5 ± 9.4 ng/g in KW) show higher Hg concentration in KW compared to the general background level of Hg as
327 defined by uncontaminated soil world reference mean Hg contents (20 to 100 ng/g; Kabata-Pendias and Pendias 2000;
328 Senesil et al. 1999; Gworek et al. 2020). However, both sites have significantly lower values compared to known
329 industrial and mining contaminated sites (> 1000 ng/g ; Kabata-Pendias and Pendias 2000; Higuera et al. 2016).
330 Nevertheless, studies conducted in different sites show a wide range of natural background Hg levels (ie. topsoils in
331 Europe, India, Brazil, Norwegian Arctic, New Zealand have values of 40, 50, 80, 110, 230 ng/g respectively (Gworek
332 et al. 2020) making it difficult to set a specific Hg threshold value for uncontaminated soil (Table S2; Figure S2c).
333 Due to the differences registered in different countries and sites of sampled soil, this indicates a link with chemical
334 and mineralogical soil properties (ie. pH, humic acid, soil grain size distribution, organic matter type and clay
335 percentage) affecting Hg in soil and its transport (O'Connor et al. 2019). Hence, we suggest that lower values in BC
336 soils are likely explained by the low clay, organic carbon and nitrogen contents (10.7 %, 4 % and 0.3 % in soil surface
337 respectively). While KW higher Hg soil contents can be explained by the higher clay proportion (66 %) and organic
338 carbon and nitrogen contents (9 % and 0.92 %). On such clay loam soils and rich organic matter, Hg binding is
339 facilitated explaining higher content (O'Connor et al. 2019). Moreover, the higher temperatures and lower
340 precipitation and altitude in KW can be responsible for a higher dry deposition from gaseous elementary Hg in the
341 forest floor (Teixeira et al. 2017).

342 In parallel, the litter showed higher Hg concentration than that in foliage in both BC (62.9 ± 17.8 ng/g) and
343 KW (75.7 ± 20.3 ng/g) (Table 1) likely explained by the process of the Hg input into the litter through foliage shedding
344 and throughfall to the forest floor (Rea et al. 1996; Pleijel et al. 2021).

345

346 **4.2. Seasonal foliage Hg content versus seasonal atmospheric Hg and CO₂**

347

348 The late winter-early spring registered the highest Hg concentration for foliage in both groves, while summer
349 and early fall to a less extent recorded the lowest concentrations (Figure 1a,b). Unexpectedly, we found a good positive
350 covariation between Hg contents of our olive tree foliage and that of the atmosphere in the Northern Hemisphere
351 (Jiskra et al. 2018). According to (Obrist, 2007), the observed maximum Hg_{atm} (from October to March) can be
352 explained by the anthropogenic and natural Hg emissions (ie. soil carbon mineralization, plant dormancy, net
353 respiration of the global forest ecosystems) exceeding Hg burial processes (ie. Photosynthetic activity and stomatal
354 conductance, forest floor Hg uptakes).

355 This author discussed the significant role of the northern hemisphere vegetation and forest floor respiration and
356 suggested that the decreasing atmospheric Hg content starting in March and reaching the minimal values in July-
357 August is likely attributable to the plant uptakes (Obrist 2007; Jiskra et al. 2018). However at our latitudes, BC and
358 KW foliage evergreen olive trees show also a decrease in Hg contents from end of March to late September, with
359 minimum values centered in August suggesting a decline of the plant Hg uptake likely explained by the reduction of
360 the stomatal conductance (Lindberg et al. 2007; Pleijel et al. 2021). This minimal photosynthetic activity occurs during
361 the driest (0 mm precipitation) and hottest temperatures (above 25°C) in our sites. While the increase of the Hg intake
362 starting in September and reaching its maximum in March occurs during the increasing Northern Hemisphere
363 atmospheric Hg (Figure 3a,b). In different Olive cultivars from Italy, Proietti and Famiani (2002) show that lowest

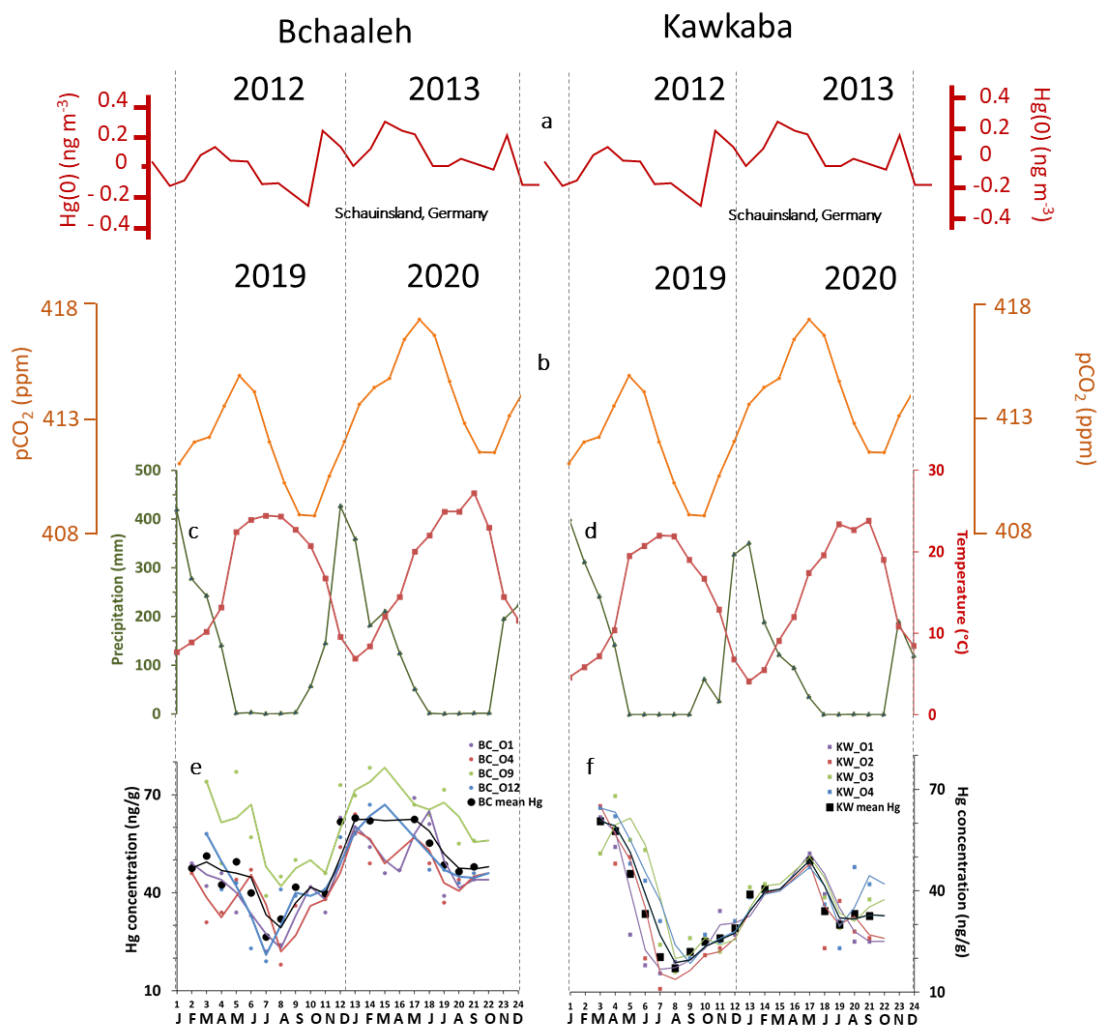


364 photosynthetic activity occur during summer (August) but also in winter (December) which is not supported by our
365 data. The positive covariation between our olive foliage and atmospheric Hg contents do not support the previous
366 cited studies showing a strong depletion of atmospheric Hg concomitant to vegetation uptake in summer period
367 uptakes (Obrist 2007; Jiskra et al. 2018). Two hypotheses can explain such positive correlations between our plant
368 foliage and air Hg concentrations. Taking into account Hg results obtained during several seasonal campaigns in the
369 surface waters of the Mediterranean Sea and the above atmospheric layer, it has been evidenced that the highest Hg
370 fluxes to the atmosphere occur mainly in summer (Kotnik et al. 2014; Wangberg et al. 2001) and a higher TGM is
371 registered in the eastern Mediterranean compared with the western Mediterranean and Northern Europe (Wängberg
372 et al., 2001). Hence, we can hypothesize that a reverse Hg seasonal cycle compared to the Northern Hemisphere values
373 would stand on a different seasonal atmospheric Hg variation than in the Northern Hemisphere.

374 On the other hand, other studies reported the same positive correlation between atmospheric Hg and crops (Niu et al.
375 2011). This suggests a second hypothesis where our groves seasonally exposed to high atmospheric Hg, accumulate
376 Hg in their foliage (Lindberg et al. 2007; Pleijel et al. 2021). According to Hanson et al. (1995), a compensation point
377 for Hg uptake by plant foliage can be considered but no information to our knowledge is available for the specific
378 case of the olive trees. The tight link between foliage Hg uptake and stomatal conductance seasonal variations can be
379 also deduced from the analysis of the partial pressure of the $p\text{CO}_{2\text{atm}}$ seasonal variation (Obrist 2007; Sprovieri et al.
380 2016; Jiskra et al. 2018; Obrist et al. 2018; Pleijel et al. 2021) (Figure 3b,e,f). Very good covariation between olive
381 foliage Hg and $p\text{CO}_{2\text{atm}}$ are shown for BC and KW despite a notable offset of one month at KW to two months at BC
382 can be deduced (Figure S3). Taking into account our calculated time lags, we obtained significant correlations between
383 our foliage Hg content and $p\text{CO}_{2\text{atm}}$ of 0.718 and 0.704 in BC and KW respectively. Interestingly a one month time-
384 lag between atmospheric Hg and $p\text{CO}_{2\text{atm}}$ is also reported by Jiskra et al. (2018) for most northern hemisphere sites.
385 The offset of one to two months between maxima of BC and KW foliage Hg (March/April) and $p\text{CO}_{2\text{atm}}$ (May)
386 suggests that the minimum of Hg in the foliage occur during the decreasing phase of the $p\text{CO}_{2\text{atm}}$ when the global
387 northern hemisphere tend to become a net sink of CO_2 . When minimum values of $p\text{CO}_{2\text{atm}}$ are reached at the end of
388 the dry summer (Figure 3b), concomitant to minimum atmospheric Hg (Figure 3a), end of the drought and increase of
389 precipitation (Figure 3c, d), BC and KW olive trees show a rise of the Hg uptake. The photosynthetic activity and
390 the stomatal conductance related to the climatic parameters (temperature, precipitation, humidity, $p\text{CO}_2$) as shown by
391 Ozturk et al. (2021) and the atmospheric Hg explain our foliage Hg seasonal cycle. At a regional scale, our sites show
392 different time lags between BC and KW that we cannot explain fully except their altitudinal differences which can
393 suggest that BC grove benefits of less drought in summer. This can also be explained by the physiology of olive trees
394 that is characterised by small foliage surface area as a response to the high temperature and less humidity in summer
395 and the stomatal conductance in the foliage that increase in winter and decrease in summer. As per (Connor & Fereres,
396 2010), olive is a day neutral plant where its reproductivity is affected by temperature and sunlight. Its vegetative growth
397 is limited by the low temperature in the winter season and water supply in the summer season. The water loss from
398 the foliage due to transpiration and temperature, creates a replacement for water source to be the soil through the roots.
399 The xylem being the main transporter between the roots and the canopy. During the day the evaporation increase and
400 the plant water content decreases and become minimal during midday, noting that the soil water content is high.



401 During the evening the olive tree seeks soil water as an equilibrium. If soil water is not available enough to cover the
 402 olive need, the evergreen olive is able to adapt through conservation of internal water especially during severe summer
 403 drought, due to its ability to restrict water loss to the atmosphere and maximize extraction of soil water. Further
 404 analysis and data are necessary to confirm the above assumption.



405 **Figure 3.** Seasonal variations of (a) atmospheric Hg(0) (Jiskra et al., 2018), (b) pCO₂ (NOAA Global Monitoring
 406 Laboratory), (c) and (d) precipitations and temperature of BC and KW respectively and (e) and (f) foliage Hg
 407 concentration in BC and KW olive groves respectively
 408
 409

410
 411
 412



413 **4.3. Hg uptake in BC and KW grove systems**

414

415 **4.3.1. Hg cycling in the stems, litter and soil system**

416

417 For each site, Hg contents in stems exhibit narrow range between the different trees except BCO9 tree showing the
418 highest values as observed for the foliage. We speculate that this higher Hg content is the adjunction of chemical
419 products as fertilizer on the plot 549 likely between fall and winter (Figure S1) belonging to different owner.

420 At a seasonal scale, the averaged Hg values of stems, litter and soil system show no statistical significance differences
421 between the four seasons for the litter and soil while stems show a significant difference between winter (lowest
422 values) and spring (p-value= 0.030) and winter-autumn (p-value= 0.047) in BC grove mostly similar to foliage
423 changes. The same behavior was registered in KW in litter and soils, while stems showing statistical significance
424 differences between autumn and spring (p-value= 0.011), spring-winter (p-value= 0.006) and spring-summer (p-
425 value= 0.004) (Table 2). Despite the small amount of Hg content in the stems, the statistically significant seasonal
426 changes may suggest that small amount of Hg move from the foliage to the lignified tissues as stems. However, we
427 cannot neglect the Hg transport in xylem sap from the roots to the aboveground plant tissues even if minimal (Yang
428 et al. 2018).

429 We can suggest the following Hg cycling in the system of the Olive grove/soil. In winter-early spring the highest
430 concentrations in foliage feed continuously the litter and can explain the following maximal spring Hg content in the
431 litter. The decomposition of the litter organic matter during the wettest conditions likely liberate Hg in the Hg(0) or
432 Hg(II) forms or MeHg either towards the atmosphere or the surface soil respectively. A fraction of the degraded
433 organic matter is transferred through gaseous evaporative processes towards the atmosphere while another fraction of
434 the Hg is lixiviated towards the deeper soil in addition to dry Hg deposition during dry season (Teixeira et al. 2017).
435 We can also speculate that the small Hg decrease observed during the winter season in BC can be due to the transport
436 of total Hg and MeHg through the roots and xylem sap to the above ground tissues.

437

438 **4.3.2. Hg uptake in foliage: atmospheric or soil sources?**

439

440 In uncontaminated sites as those presented in this study, no significant correlation between the foliage and soil Hg
441 content is observed in agreement with Higuera et al. (2012). In contrary, contaminated sites, exhibit a good correlation
442 (Higuera et al. 2016). Interestingly, in the Mediterranean region, it is reported that intensity of mycorrhizal
443 colonization of olive tree roots increase with the increase of seasonal precipitation and decreased with the increase of
444 air temperature (Meddad-Hamza et al. 2017). This is an independent argument to support the atmosphere being the
445 main Hg source to the foliage during the wet seasons, but also confirming in absence of mycorrhizal activity a possible
446 minimal Hg uptake from the soil to the foliage and stems through water during the drought season (Rea et al. 2002;
447 Meddad-Hamza et al. 2017). Eventually, we suggest that the main source of Hg for both olive groves is the atmospheric
448 mercury.

449



450 5. Conclusion

451
452 This is the first study conducted on monumental olive trees in a non-contaminated site of the MENA region and
453 followed at a monthly basis over 18 months. Findings of our study in remote and uncontaminated sites indicate a
454 higher uptake of Hg in the olive foliage compared to stems, fruits items and a remarkable Hg_F seasonal variation in
455 both studied groves. Winter and Spring were particularly suitable for Hg accumulation in foliage in both sites. The
456 significant correlation between our foliage Hg contents and the atmospheric Hg content and pCO_2 , despite the one to
457 two months' time lag, suggests that 1) the main source of foliage Hg is the atmospheric Hg 2) the main factor
458 explaining the seasonal Hg accumulation in foliage is due to the photosynthetic activity and stomatal conductance,
459 but it can also be due to the physiology of olive trees. Thus, a more intensive study on the physiology of olive tree
460 must be focused on, and more intensive studies on foliage, soil and litter is needed to be able to assess the source of
461 Hg uptake in the olive trees. However further comparison and studies on the seasonal atmospheric Hg in the eastern
462 Mediterranean basin are necessary to test our hypothesis of the reversed seasonality of Hg since contrary to the global
463 Northern Hemisphere vegetation, our olive groves act as a sink of Hg and CO_2 when global Northern vegetation is
464 emitting and vice-versa. This relationship $Hg_F - Hg_{atm} - pCO_{2atm}$ should be further investigated along the season and
465 locally to better understand the observed time lags. Soil surface registered the highest Hg concentration among all
466 studied compartments due to well-known processes of litter and throughfall. Moreover, this study highlights
467 significant differences between Hg soil groves due to differences in soil characteristics. In this study we worked on
468 the present in order to have a better understanding of the Hg cycle in the olive tree. A second step would be to
469 reconstruct the paleo-evolution through also studying tree rings Hg concentration were we can also identify a seasonal
470 variation. Our main contribution in this study is to see how the present-day olive trees records some elements such as
471 Hg to better understand the Hg in tree rings for the past.

472

473 Data availability

474 The datasets generated during and/or analyzed during the current study are available from the corresponding author
475 on reasonable request.

476

477 Author Contributions

478 The corresponding author **Ilham Bentaleb** is responsible for ensuring that the descriptions are accurate and agreed upon
479 by all authors. Conceptualization and methodology were done and developed by **Ilham Bentaleb** and **Lamis Chalak**.
480 The material collection was performed by **Naghm Tabaja**, **Ilham Bentaleb**, **Lamis Chalak**, **Ihab Jomaa**, and **Milad**
481 **Riachy**. Sample storage and preparation in Lebanon organized by **Naghm Tabaja**. Material preparation at ISEM by
482 **Naghm Tabaja**. Data collection and analysis were performed by **Naghm Tabaja**, **Ilham Bentaleb**, **David Amouroux**,
483 and **Emmanuel Tessier**. The setting of the meteorological stations by **Ihab Jomaa**. Subsamples of soil were analyzed
484 for carbon and nitrogen elemental contents (%) by **François Fourel**. The first draft of the manuscript was written by
485 **Naghm Tabaja**. **Ilham Bentaleb**, **Lamis Chalak**, **David Amouroux**, **Ihab Jomaa**, and **Milad Riachy** commented
486 on previous versions of the manuscript. All authors read and approved the final manuscript. Supervision was done by
487 **Ilham Bentaleb** and **Lamis Chalak**.

488

489 Competing interests

490 The authors declare that they have no known competing financial interests or personal relationships that could have
491 appeared to influence the work reported in this paper.



492

493

494

Acknowledgments

495

496

497

498

499

500

501

502

503

504

505

506

Funding

507

508

509

510

511

References

512

513

514

515

516

517

518

519

520

521

522

523

524

525

526

Abou Habib, N., Taleb, M., & Khoury, R. (2015). ENVIRONMENTAL AND SOCIAL SAFEGUARD STUDIES FOR LAKE QARAOUN POLLUTION PREVENTION PROJECT. VI(E4749).

Assad, M. (2017). Transfert des éléments traces métalliques vers les végétaux: Mécanismes et évaluations des risques dans des environnements exposés à des activités anthropiques [Bourgogne Franche-Comté. Sciences agricoles.]. <https://tel.archives-ouvertes.fr/tel-01787667>.

Baayoun, A., Itani, W., El Helou, J., Halabi, L., Medlej, S., El Malki, M., Moukhadder, A., Aboujaoude, L. K., Kabakian, V., Mounajed, H., Mokalled, T., Shihadeh, A., Lakkis, I., & Saliba, N. A. (2019). Emission inventory of key sources of air pollution in Lebanon. *Atmospheric Environment*, 215, 116871. <https://doi.org/10.1016/j.atmosenv.2019.116871>

Badr, R., Holail, H., & Olama, Z. (2014). WATER QUALITY ASSESSMENT OF HASBANI RIVER IN SOUTH LEBANON: MICROBIOLOGICAL AND CHEMICAL CHARACTERISTICS AND THEIR IMPACT ON THE ECOSYSTEM. 3, 16.

Bargagli, R. (1995). The elemental composition of vegetation and the possible incidence of soil contamination of samples. *Science of The Total Environment*, 176(1–3), 121–128. [https://doi.org/10.1016/0048-9697\(95\)04838-3](https://doi.org/10.1016/0048-9697(95)04838-3)



- 527 Barre, J. P. G., Deletraz, G., Sola-Larrañaga, C., Santamaria, J. M., Bérail, S., Donard, O. F. X., & Amouroux, D.
528 (2018). Multi-element isotopic signature (C, N, Pb, Hg) in epiphytic lichens to discriminate atmospheric
529 contamination as a function of land-use characteristics (Pyrénées-Atlantiques, SW France). *Environmental*
530 *Pollution*, 243, 961–971. <https://doi.org/10.1016/j.envpol.2018.09.003>
- 531 Bishop, K. H., Lee, Y.-H., Munthe, J., & Dambrine, E. (1998). Xylem sap as a pathway for total mercury and
532 methylmercury transport from soils to tree canopy in the boreal forest. *Biogeochemistry*, 40, 101–113.
- 533 Bishop, K., Shanley, J. B., Riscassi, A., de Wit, H. A., Eklöf, K., Meng, B., Mitchell, C., Osterwalder, S., Schuster,
534 P. F., Webster, J., & Zhu, W. (2020). Recent advances in understanding and measurement of mercury in the
535 environment: Terrestrial Hg cycling. *Science of The Total Environment*, 721, 137647.
536 <https://doi.org/10.1016/j.scitotenv.2020.137647>
- 537 Blackwell, B. D., & Driscoll, C. T. (2015). Using foliar and forest floor mercury concentrations to assess spatial
538 patterns of mercury deposition. *Environmental Pollution*, 202, 126–134.
539 <https://doi.org/10.1016/j.envpol.2015.02.036>
- 540 Boening, D. W. (2000). Ecological effects, transport, and fate of mercury: A general review. 17.
- 541 Borjac, J., El Joumaa, M., Kawach, R., Youssef, L., & Blake, D. A. (2019). Heavy metals and organic compounds
542 contamination in leachates collected from Deir Kanoun Ras El Ain dump and its adjacent canal in South
543 Lebanon. *Heliyon*, 5(8), e02212. <https://doi.org/10.1016/j.heliyon.2019.e02212>
- 544 Borjac, J., El Joumaa, M., Youssef, L., Kawach, R., & Blake, D. A. (2020). Quantitative Analysis of Heavy Metals
545 and Organic Compounds in Soil from Deir Kanoun Ras El Ain Dump, Lebanon. *The Scientific World*
546 *Journal*, 2020, 1–10. <https://doi.org/10.1155/2020/8151676>
- 547 Briffa, J., Sinagra, E., & Blundell, R. (2020). Heavy metal pollution in the environment and their toxicological
548 effects on humans. *Heliyon*, 6(9), e04691. <https://doi.org/10.1016/j.heliyon.2020.e04691>
- 549 Cavallini, A., Natali, L., Durante, M., & Maserti, B. (1999). Mercury uptake, distribution and DNA affinity in
550 durum wheat (*Triticum durum* Desf.) plants. *Science of The Total Environment*, 243–244, 119–127.
551 [https://doi.org/10.1016/S0048-9697\(99\)00367-8](https://doi.org/10.1016/S0048-9697(99)00367-8)
- 552 Clarkson, T. W., & Magos, L. (2006). The Toxicology of Mercury and Its Chemical Compounds. *Critical Reviews*
553 *in Toxicology*, 36(8), 609–662. <https://doi.org/10.1080/10408440600845619>



- 554 Connor, D. J., & Fereres, E. (2010). The Physiology of Adaptation and Yield Expression in Olive. In J. Janick (Ed.),
555 Horticultural Reviews (pp. 155–229). John Wiley & Sons, Inc. <https://doi.org/10.1002/9780470650882.ch4>
- 556 Duval, B., Gredilla, A., Fdez-Ortiz de Vallejuelo, S., Tessier, E., Amouroux, D., & de Diego, A. (2020). A simple
557 determination of trace mercury concentrations in natural waters using dispersive Micro-Solid phase
558 extraction preconcentration based on functionalized graphene nanosheets. *Microchemical Journal*, 154,
559 104549. <https://doi.org/10.1016/j.microc.2019.104549>
- 560 EJOLT. (2019). Cimenterie Nationale Factory in Chekaa, Lebanon | EJAtlas. Environmental Justice Atlas.
561 <https://ejatlas.org/conflict/chekaa>
- 562 Ermolin, M. S., Fedotov, P. S., Malik, N. A., & Karandashev, V. K. (2018). Nanoparticles of volcanic ash as a
563 carrier for toxic elements on the global scale. *Chemosphere*, 200, 16–22.
564 <https://doi.org/10.1016/j.chemosphere.2018.02.089>
- 565 FREEMAN, M., & CARLSON, R. M. (2005). ESSENTIAL NUTRIENTS. *Olive Production Manual*, 3353, 75.
- 566 Gårdfeldt, K., Sommar, J., Ferrara, R., Ceccarini, C., Lanzillotta, E., Munthe, J., Wängberg, I., Lindqvist, O.,
567 Pirrone, N., Sprovieri, F., Pesenti, E., & Strömberg, D. (2003). Evasion of mercury from coastal and open
568 waters of the Atlantic Ocean and the Mediterranean Sea. *Atmospheric Environment*, 37, 73–84.
569 [https://doi.org/10.1016/S1352-2310\(03\)00238-3](https://doi.org/10.1016/S1352-2310(03)00238-3)
- 570 Gérard, J., & Nehmé, C. (2020). Lebanon. Méditerranée. *Revue Géographique Des Pays Méditerranéens / Journal of*
571 *Mediterranean Geography*, 131, Article 131. <https://journals.openedition.org/mediterranee/11018#>
- 572 Grigal, D. (2003). Mercury Sequestration in Forests and Peatlands: A Review. *Journal of Environmental Quality - J*
573 *ENVIRON QUAL*, 32. <https://doi.org/10.2134/jeq2003.0393>
- 574 Gworek, B., Dmuchowski, W., & Baczevska-Dąbrowska, A. H. (2020). Mercury in the terrestrial environment: A
575 review. *Environmental Sciences Europe*, 32(1), 128. <https://doi.org/10.1186/s12302-020-00401-x>
- 576 Hanson, P. J., Lindberg, S. E., Tabberer, T. A., Owens, J. G., & Kim, K.-H. (1995). Foliar exchange of mercury
577 vapor: Evidence for a compensation point. *Water, Air, & Soil Pollution*, 80(1–4), 373–382.
578 <https://doi.org/10.1007/BF01189687>
- 579 Higuera, P., Amorós, J. A., Esbrí, J. M., García-Navarro, F. J., Pérez de los Reyes, C., & Moreno, G. (2012). Time
580 and space variations in mercury and other trace element contents in olive trees from the Almadén Hg-



- 581 mining district. *Journal of Geochemical Exploration*, 123, 143–151.
- 582 <https://doi.org/10.1016/j.gexplo.2012.04.012>
- 583 Higuera, P. L., Amorós, J. Á., Esbrí, J. M., Pérez-de-los-Reyes, C., López-Berdonces, M. A., & García-Navarro, F.
- 584 J. (2016a). Mercury transfer from soil to olive trees. A comparison of three different contaminated sites.
- 585 *Environmental Science and Pollution Research*, 23(7), 6055–6061. [https://doi.org/10.1007/s11356-015-](https://doi.org/10.1007/s11356-015-4357-2)
- 586 4357-2
- 587 Higuera, P. L., Amorós, J. Á., Esbrí, J. M., Pérez-de-los-Reyes, C., López-Berdonces, M. A., & García-Navarro, F.
- 588 J. (2016b). Mercury transfer from soil to olive trees. A comparison of three different contaminated sites.
- 589 *Environmental Science and Pollution Research*, 23(7), 6055–6061. [https://doi.org/10.1007/s11356-015-](https://doi.org/10.1007/s11356-015-4357-2)
- 590 4357-2
- 591 Jindrich Petrik, Kodeih, N., IndyACT, Arnika Association, & IPEN WG. (2013). Mercury in Fish and Hair Samples
- 592 from Batroun, Lebanon. <https://doi.org/10.13140/RG.2.2.12052.40327>
- 593 Jiskra, M., Sonke, J. E., Obrist, D., Bieser, J., Ebinghaus, R., Myhre, C. L., Pfaffhuber, K. A., Wängberg, I.,
- 594 Kyllönen, K., Worthy, D., Martin, L. G., Labuschagne, C., Mkololo, T., Ramonet, M., Magand, O., &
- 595 Dommergue, A. (2018a). A vegetation control on seasonal variations in global atmospheric mercury
- 596 concentrations. *Nature Geoscience*, 11(4), 244–250. <https://doi.org/10.1038/s41561-018-0078-8>
- 597 Jiskra, M., Sonke, J. E., Obrist, D., Bieser, J., Ebinghaus, R., Myhre, C. L., Pfaffhuber, K. A., Wängberg, I.,
- 598 Kyllönen, K., Worthy, D., Martin, L. G., Labuschagne, C., Mkololo, T., Ramonet, M., Magand, O., &
- 599 Dommergue, A. (2018b). A vegetation control on seasonal variations in global atmospheric mercury
- 600 concentrations. *Nature Geoscience*, 11(4), 244–250. <https://doi.org/10.1038/s41561-018-0078-8>
- 601 Jurdi, M., Korfali, S. I., Karahagopian, Y., & Davies, B. E. (2002). Evaluation of Water Quality of the Qaraaoun
- 602 Reservoir, Lebanon: Suitability for Multipurpose Usage. 77(11–30), 20.
- 603 Kabata-Pendias, A., & Pendias, H. (2000). Trace elements in soils and plants (3rd ed). CRC Press.
- 604 Kobrossi, R., Nuwayhid, I., Sibai, A. M., El-Fadel, M., & Khogali, M. (2002). Respiratory health effects of
- 605 industrial air pollution on children in North Lebanon. *International Journal of Environmental Health*
- 606 *Research*, 12(3), 205–220. <https://doi.org/10.1080/09603/202/000000970>



- 607 Kotnik, J., Sprovieri, F., Ogrinc, N., Horvat, M., & Pirrone, N. (2014). Mercury in the Mediterranean, part I: Spatial
608 and temporal trends. *Environmental Science and Pollution Research*, 21(6), 4063–4080.
609 <https://doi.org/10.1007/s11356-013-2378-2>
- 610 Lebanon: Air Pollution | IAMAT. (2020). <https://www.iamat.org/country/lebanon/risk/air-pollution>
- 611 Li, D., Fang, K., Li, Y., Chen, D., Liu, X., Dong, Z., Zhou, F., Guo, G., Shi, F., Xu, C., & Li, Y. (2017). Climate,
612 intrinsic water-use efficiency and tree growth over the past 150 years in humid subtropical China. *PLOS*
613 *ONE*, 12(2), e0172045. <https://doi.org/10.1371/journal.pone.0172045>
- 614 Lindberg, S., Bullock, R., Ebinghaus, R., Engstrom, D., Feng, X., Fitzgerald, W., Pirrone, N., Prestbo, E., &
615 Seigneur, C. (2007). A Synthesis of Progress and Uncertainties in Attributing the Sources of Mercury in
616 Deposition. *Ambio*, 36(1), 19–32.
- 617 Lodenius, M., Tulisalo, E., & Soltanpour-Gargari, A. (2003). Exchange of mercury between atmosphere and
618 vegetation under contaminated conditions. *Science of The Total Environment*, 304(1–3), 169–174.
619 [https://doi.org/10.1016/S0048-9697\(02\)00566-1](https://doi.org/10.1016/S0048-9697(02)00566-1)
- 620 Luo, Y., Duan, L., Driscoll, C. T., Xu, G., Shao, M., Taylor, M., Wang, S., & Hao, J. (2016). Foliage/atmosphere
621 exchange of mercury in a subtropical coniferous forest in south China. *Journal of Geophysical Research:*
622 *Biogeosciences*, 121(7), 2006–2016. <https://doi.org/10.1002/2016JG003388>
- 623 Maillard, F., Girardclos, O., Assad, M., Zappellini, C., Pérez Mena, J. M., Yung, L., Guyeux, C., Chrétien, S.,
624 Bigham, G., Cosio, C., & Chalot, M. (2016). Dendrochemical assessment of mercury releases from a pond
625 and dredged-sediment landfill impacted by a chlor-alkali plant. *Environmental Research*, 148, 122–126.
626 <https://doi.org/10.1016/j.envres.2016.03.034>
- 627 Meddad-Hamza, A., Hamza, N., Neffar, S., Beddiar, A., Gianinazzi, S., & Chenchouni, H. (2017). Spatiotemporal
628 variation of arbuscular mycorrhizal fungal colonization in olive (*Olea europaea* L.) roots across a broad
629 mesic-xeric climatic gradient in North Africa. *Science of The Total Environment*, 583, 176–189.
630 <https://doi.org/10.1016/j.scitotenv.2017.01.049>
- 631 Naharro, R., Esbri, J., Amorós, J., & Higuera, P. (2018). Atmospheric mercury uptake and desorption from olive-
632 tree leaves. 20(EGU2018-2982,2018), 2.



- 633 Nassif, N., Jaoude, L. A., El Hage, M., & Robinson, C. A. (2016). Data Exploration and Reconnaissance to Identify
634 Ocean Phenomena: A Guide for <i>In Situ&/i> Data Collection. *Journal of Water Resource and*
635 *Protection*, 08(10), 929–943. <https://doi.org/10.4236/jwarp.2016.810076>
- 636 Niu, Z., Zhang, X., Wang, Z., & Ci, Z. (2011). Field controlled experiments of mercury accumulation in crops from
637 air and soil. *Environmental Pollution*, 159(10), 2684–2689. <https://doi.org/10.1016/j.envpol.2011.05.029>
- 638 Obrist, D. (2007). Atmospheric mercury pollution due to losses of terrestrial carbon pools? *Biogeochemistry*, 85(2),
639 119–123. <https://doi.org/10.1007/s10533-007-9108-0>
- 640 Obrist, D., Kirk, J. L., Zhang, L., Sunderland, E. M., Jiskra, M., & Selin, N. E. (2018). A review of global
641 environmental mercury processes in response to human and natural perturbations: Changes of emissions,
642 climate, and land use. *Ambio*, 47(2), 116–140. <https://doi.org/10.1007/s13280-017-1004-9>
- 643 O'Connor, D., Hou, D., Ok, Y. S., Mulder, J., Duan, L., Wu, Q., Wang, S., Tack, F. M. G., & Rinklebe, J. (2019a).
644 Mercury speciation, transformation, and transportation in soils, atmospheric flux, and implications for risk
645 management: A critical review. *Environment International*, 126, 747–761.
646 <https://doi.org/10.1016/j.envint.2019.03.019>
- 647 Ozturk, M., Altay, V., Gönenç, T. M., Unal, B. T., Efe, R., Akçiçek, E., & Bukhari, A. (2021). An Overview of
648 Olive Cultivation in Turkey: Botanical Features, Eco-Physiology and Phytochemical Aspects. *Agronomy*,
649 11(2), 295. <https://doi.org/10.3390/agronomy11020295>
- 650 Patra, M., & Sharma, A. (2000). Mercury toxicity in plants. *The Botanical Review*, 66(3), 379–422.
651 <https://doi.org/10.1007/BF02868923>
- 652 Pleijel, H., Klingberg, J., Nerentorp, M., Broberg, M. C., Nyirambangutse, B., Munthe, J., & Wallin, G. (2021).
653 Mercury accumulation in leaves of different plant types – the significance of tissue age and specific leaf
654 area [Preprint]. *Biogeochemistry: Air - Land Exchange*. <https://doi.org/10.5194/bg-2021-117>
- 655 Proietti, P., & Famiani, F. (2002). Diurnal and Seasonal Changes in Photosynthetic Characteristics in Different
656 Olive (*Olea europaea* L.) Cultivars. *Photosynthetica*, 40(2), 171–176.
657 <https://doi.org/10.1023/A:1021329220613>
- 658 Rea, A. W., Keeler, G. J., & Scherbatskoy, T. (1996). The deposition of mercury in throughfall and litterfall in the
659 lake champlain watershed: A short-term study. *Atmospheric Environment*, 30(19), 3257–3263.
660 [https://doi.org/10.1016/1352-2310\(96\)00087-8](https://doi.org/10.1016/1352-2310(96)00087-8)



- 661 Rea, A. W., Lindberg, S. E., Scherbatskoy, T., & Keeler, G. J. (2002). Mercury Accumulation in Foliage over Time
662 in Two Northern Mixed-Hardwood Forests. 19.
- 663 Schneider, L., Allen, K., Walker, M., Morgan, C., & Haberle, S. (2019). Using Tree Rings to Track Atmospheric
664 Mercury Pollution in Australia: The Legacy of Mining in Tasmania. *Environmental Science & Technology*,
665 53(10), 5697–5706. <https://doi.org/10.1021/acs.est.8b06712>
- 666 Schwesig, D., & Krebs, O. (2003). The role of ground vegetation in the uptake of mercury and methylmercury in a
667 forest ecosystem. *Plant and Soil*, 11.
- 668 Senesil, G. S., Baldassarre, G., Senesi, N., & Radina, B. (1999). Trace element inputs into soils by anthropogenic
669 activities and implications for human health. *Chemosphere*, 39(2), 343–377. [https://doi.org/10.1016/S0045-](https://doi.org/10.1016/S0045-6535(99)00115-0)
670 [6535\(99\)00115-0](https://doi.org/10.1016/S0045-6535(99)00115-0)
- 671 Sghaier, A., Perttunen, J., Sievaänen, R., Boujnah, D., Ouessar, M., Ben Ayed, R., & Naggaz, K. (2019).
672 Photosynthetic activity modelisation of olive trees growing under drought conditions. *Scientific Reports*,
673 9(1), 15536. <https://doi.org/10.1038/s41598-019-52094-9>
- 674 Sprovieri, F., Pirrone, N., Bencardino, M., D'Amore, F., Carbone, F., Cinnirella, S., Mannarino, V., Landis, M.,
675 Ebinghaus, R., Weigelt, A., Brunke, E.-G., Labuschagne, C., Martin, L., Munthe, J., Wängberg, I., Artaxo,
676 P., Morais, F., Barbosa, H. de M. J., Brito, J., ... Norstrom, C. (2016). Atmospheric mercury concentrations
677 observed at ground-based monitoring sites globally distributed in the framework of the GMOS network.
678 *Atmospheric Chemistry and Physics*, 16(18), 11915–11935. <https://doi.org/10.5194/acp-16-11915-2016>
- 679 Teixeira, D. C., Lacerda, L. D., & Silva-Filho, E. V. (2017). Mercury sequestration by rainforests: The influence of
680 microclimate and different successional stages. *Chemosphere*, 168, 1186–1193.
681 <https://doi.org/10.1016/j.chemosphere.2016.10.081>
- 682 Terral, J.-F., Alonso, N., Capdevila, R. B. i, Chatti, N., Fabre, L., Fiorentino, G., Marinval, P., Jordá, G. P., Pradat,
683 B., Rovira, N., & Alibert, P. (2004). Historical biogeography of olive domestication (*Olea europaea* L.) as
684 revealed by geometrical morphometry applied to biological and archaeological material: Historical
685 biogeography of olive domestication (*Olea europaea* L.). *Journal of Biogeography*, 31(1), 63–77.
686 <https://doi.org/10.1046/j.0305-0270.2003.01019.x>
- 687 Tomiyasu, T., Matsuo, T., Miyamoto, J., Imura, R., Anazawa, K., & Sakamoto, H. (2005). Low level mercury
688 uptake by plants from natural environments—Mercury distribution in *Solidago altissima* L.-.



- 689 Environmental Sciences: An International Journal of Environmental Physiology and Toxicology, 12(4),
690 231–238.
- 691 UNEP. (2019). Technical Background Report to the Global Mercury Assessment 2018. IVL Svenska Miljöinstitutet.
- 692 Wang, X., Lin, C.-J., Lu, Z., Zhang, H., Zhang, Y., & Feng, X. (2016). Enhanced accumulation and storage of
693 mercury on subtropical evergreen forest floor: Implications on mercury budget in global forest ecosystems:
694 HG STORAGE ON SUBTROPICAL FOREST FLOOR. *Journal of Geophysical Research: Biogeosciences*, 121(8), 2096–2109. <https://doi.org/10.1002/2016JG003446>
- 695
- 696 Wängberg, I., Munthe, J., Pirrone, N., Iverfeldt, Å., Bahlman, E., Costa, P., Ebinghaus, R., Feng, X., Ferrara, R.,
697 Gärdfeldt, K., Kock, H., Lanzillotta, E., Mamane, Y., Mas, F., Melamed, E., Osnat, Y., Prestbo, E.,
698 Sommar, J., Schmolke, S., ... Tuncel, G. (2001). Atmospheric mercury distribution in Northern Europe and
699 in the Mediterranean region. *Atmospheric Environment*, 35(17), 3019–3025.
700 [https://doi.org/10.1016/S1352-2310\(01\)00105-4](https://doi.org/10.1016/S1352-2310(01)00105-4)
- 701 Wofsy, S. C., Goulden, M. L., Munger, J. W., Fan, S.-M., Bakwin, P. S., Daube, B. C., Bassow, S. L., & Bazzaz, F.
702 A. (1993). Net Exchange of CO₂ in a Mid-Latitude Forest. *Science*, 260(5112), 1314–1317.
703 <https://doi.org/10.1126/science.260.5112.1314>
- 704 Wohlgenuth, L., Rautio, P., Ahrends, B., Russ, A., Vesterdal, L., Waldner, P., Timmermann, V., Eickenscheidt, N.,
705 Fürst, A., Greve, M., Roskams, P., Thimonier, A., Nicolas, M., Kowalska, A., Ingerslev, M., Merilä, P.,
706 Benham, S., Jacoban, C., Hoch, G., ... Jiskra, M. (2021). Physiological and climate controls on foliar
707 mercury uptake by European tree species [Preprint]. *Biogeochemistry: Air - Land Exchange*.
708 <https://doi.org/10.5194/bg-2021-239>
- 709 Wright, L. P., Zhang, L., & Marsik, F. J. (2016). Overview of mercury dry deposition, litterfall, and throughfall
710 studies. *Atmospheric Chemistry and Physics*, 16(21), 13399–13416. [https://doi.org/10.5194/acp-16-13399-](https://doi.org/10.5194/acp-16-13399-2016)
711 2016
- 712 Yammine, P., Kfoury, A., El-Khoury, B., Nouali, H., El-Nakat, H., Ledoux, F., Courcot, D., & Aboukais, A. (2010).
713 A PRELIMINARY EVALUATION OF THE INORGANIC CHEMICAL COMPOSITION OF
714 ATMOSPHERIC TSP IN THE SELAATA REGION, NORTH LEBANON. *Lebanese Science Journal*,
715 11(1), 18.



- 716 Yanai, R. D., Yang, Y., Wild, A. D., Smith, K. T., & Driscoll, C. T. (2020). New Approaches to Understand
717 Mercury in Trees: Radial and Longitudinal Patterns of Mercury in Tree Rings and Genetic Control of
718 Mercury in Maple Sap. *Water, Air, & Soil Pollution*, 231(5), 248. [https://doi.org/10.1007/s11270-020-](https://doi.org/10.1007/s11270-020-04601-2)
719 04601-2
- 720 Yang, Y., Yanai, R. D., Driscoll, C. T., Montesdeoca, M., & Smith, K. T. (2018a). Concentrations and content of
721 mercury in bark, wood, and leaves in hardwoods and conifers in four forested sites in the northeastern
722 USA. *PLOS ONE*, 13(4), e0196293. <https://doi.org/10.1371/journal.pone.0196293>
- 723 Yang, Y., Yanai, R. D., Driscoll, C. T., Montesdeoca, M., & Smith, K. T. (2018b). Concentrations and content of
724 mercury in bark, wood, and leaves in hardwoods and conifers in four forested sites in the northeastern
725 USA. *PLOS ONE*, 13(4), e0196293. <https://doi.org/10.1371/journal.pone.0196293>
- 726 Yazbeck, E. B., Rizk, G. A., Hassoun, G., El-Khoury, R., & Geagea, L. (2018). Ecological characterization of
727 ancient olive trees in Lebanon- Bshaaleh area and their age estimation. 11(2 Ver. 1), 35–44.
- 728 Zhou, J., Obrist, D., Dastoor, A., Jiskra, M., & Ryjkov, A. (2021). Vegetation uptake of mercury and impacts on
729 global cycling. *Nature Reviews Earth & Environment*, 2(4), 269–284. [https://doi.org/10.1038/s43017-021-](https://doi.org/10.1038/s43017-021-00146-y)
730 00146-y
- 731 Zhou, J., Wang, Z., & Zhang, X. (2018). Deposition and Fate of Mercury in Litterfall, Litter, and Soil in Coniferous
732 and Broad-Leaved Forests. *Journal of Geophysical Research: Biogeosciences*, 123(8), 2590–2603.
733 <https://doi.org/10.1029/2018JG004415>
- 734
735